



Mixed discrete least square meshless method for solution of quadratic partial differential equations

S. Faraji*, M.H. Afshar and J. Amani

School of Civil Engineering, Iran University of Science and Technology, Narmak, Tehran, P.O. Box 16765-163, Iran.

Received 28 July 2012; received in revised form 22 April 2013; accepted 25 June 2013

KEYWORDS

Discrete least squares
 meshless;
 Quadratic partial
 differential equations;
 Moving least squares;
 Mixed meshless;
 Irreducible meshless.

Abstract. In this paper, the Mixed Discrete Least Squared Meshless (MDLSM) method is used for solving quadratic Partial Differential Equations (PDEs). In the MDLSM method, the domain is discretized only with nodes, and a minimization of a least squares functional is carried out. The least square functional is defined as the sum of the residuals of the governing differential equation and its boundary condition at the nodal points. In MDLSM, the main unknown parameter and its first derivatives are approximated independently with the same Moving Least Squares (MLS) shape functions. The solution of the quadratic PDE does not, therefore, require calculation of the complex second order derivatives of MLS shape functions. Furthermore, both Neumann and Dirichlet boundary conditions can be treated and imposed as a Dirichlet type boundary condition, which is applied using a penalty method. The accuracy and efficiency of the MDLSM method are tested against three numerical benchmark examples from one-dimensional and two-dimensional PDEs. The results are produced and compared with the irreducible DLSP method and exact analytical solutions, indicating the ability and efficiency of the MDLSM method in efficient and effective solution of quadratic PDEs.

© 2014 Sharif University of Technology. All rights reserved.

1. Introduction

In recent years, meshless methods have been widely developed for solving Partial Differential Equations (PDEs). These methods do not need any element nor any certain connectivity, leading to a numerical method with reduced discretization costs [1]. Some familiar meshless methods include: the Smoothed Particle Hydrodynamic (SPH) method [2], the Element Free Galerkin (EFG) method [3,4], the Meshless Local Petrov–Galerkin (MLPG) method [5–8], the Reproducing Kernel Particle Method (RKPM) [9], the Local Boundary Integral Equation (LBIE) method [10,11], the hp-Meshless cloud method [12] and the Finite

Point Method (FPM) [13]. The Discrete Least Squares Meshless (DLSP) method was also proposed by Arzani and Afshar [14].

Meshless methods are categorized in two major forms: weak and strong. In contrast to the strong form that uses an original form of governing differential equation, the weak form uses an integral form obtained by the weighted residual method. A numerical integration procedure is, therefore, required for meshless methods using weak forms, such as EFG and MLPG, imposing noticeable computational cost. Furthermore, this requires the use of a background mesh for numerical integration, leading to the fact that the methods using the weak form are not truly meshless methods. The use of strong forms, however, removes the need for numerical integration and the use of background mesh, making these methods more efficient.

Minimization of the least squares functional is the

*. Corresponding author. Tel: +98 914-4918-969
 E-mail addresses: saebfaraji@civileng.iust.ac.ir (S. Faraji);
 mhafshar@iust.ac.ir (M.H. Afshar); jamani@iust.ac.ir (J.
 Amani)

basis of the DLSM method, which is defined as the sum of the residuals of the governing differential equation and its boundary condition at the nodal points. Since the DLSM method uses the strong form of governing equation, time consuming numerical integration computation is avoided. This method has shown to possess some important abilities in the solution of fluid and solid mechanics problems. After the work of Arzani and Afshar [14], for the solution of Poisson's equations, the DLSM was used for the solution of elliptic partial differential equations [15], hyperbolic problems [16] transient and steady-state [17,18] and planar elasticity [19] problems. Recently, adaptive versions of DLSM have been used for the efficient solution of fluid flow [20] and solid mechanics [1,21] problems. More lately, the MDLSM method was proposed by Amani et al. [22] and used for the solution of elasticity problems.

The concept of irreducible and mixed formulations has its origin in finite element methods. The basis of these formulations depends on the set of differential equations from which we start the discretization process. If we start with an equation system from which none of the unknown parameters can be eliminated, still leaving a well-defined problem, the formulation will be termed irreducible. With irreducible formulation, the gradients of the main unknown parameter are obtained via a post-processing of the main unknown parameters, once these parameters are calculated. If this is not the case, the formulation will be called a mixed one, in which both main unknown parameters and their gradients are approximated simultaneously and independently, leading to more accurate results. This is, in particular, for gradient type parameters, such as stresses, in elasticity problems. Furthermore, the use of mixed formulation reduces the order of shape function derivatives to half, with twofold merit. First, the order of basic functions for the construction of MLS shape functions is reduced and, second, the costly operation of constructing the complex higher order derivatives of the MLS shape function is eliminated.

In the finite element method, Zienkiewicz et al. [23,24] used mixed formulation for patch test analysis. Papadopoulos and Taylor [25] applied this formulation for contact problems. Pitkaranta and Stenberg [26] discussed the use of mixed formulation for plane elasticity problems. Raviart and Thomas [27] used a mixed method for elliptic problems. Tchonkova and Strue [28] developed the mixed least square finite element method for solving linear elasticity problems. In the context of meshless methods, Atluri et al. [29] was the first to suggest the meshless local Petrov-Galerkin mixed method for elasticity problems. The mixed meshless formulation was also applied by Soric and Jarak [30] for the analysis of shell-like structures.

More recently, Amani et al. [22] proposed the MDLSM method for planar elasticity problems.

The MDLSM method is used in this paper for the effective solution of quadratic Partial Differential Equations (PDEs). In the MDLSM method, the domain is discretized only with nodes, and a minimization of a least squares functional is carried out. The least squares functional is defined as the sum of the residuals of the governing differential equation and its boundary conditions at the nodal points. In MDLSM, the main unknown parameter and its derivatives are approximated independently with the same Moving Least Squares (MLS) shape functions. Furthermore, both the Neumann and Dirichlet boundary conditions can be treated and imposed as a Dirichlet type boundary condition, which is applied using a penalty method. The accuracy and efficiency of the MDLSM method are tested against three numerical benchmark examples from one-dimensional and two-dimensional PDEs. The results are produced and compared with the irreducible DLSM method and exact analytical solutions, indicating the ability and efficiency of the MDLSM method for the efficient and effective solution of quadratic PDEs. This paper is organized as follows: In Section 2, the MLS approximation used for shape function construction is defined. In Section 3, MDLSM formulation for solving quadratic partial differential equations is formulated. Numerical examples are solved in Section 4. Finally, some significant conclusions are summarized in Section 5.

2. Moving least square approximation method

Construction of the shape functions for approximation of unknown parameters is the main idea in meshless methods. Several approximation and interpolation methods are used for construction of the shape functions, such as Radial Basis Function (RBF) [31], Moving Kriging (MK) [32], Partition of Unity (PU) [33], Maximum Entropy (Max-Ent) [34], Local Maximum Entropy (LME) [35] and Moving Least Squares (MLS) [36]. MLS is the most popular approximation method for construction of shape functions in meshless methods [21]. Construction of the MLS shape function starts with the following approximation of the function, defined as:

$$\mathbf{u}(\mathbf{X}) = \sum_{i=1}^k p_i(\mathbf{X}) a_i(\mathbf{X}) = \mathbf{P}^T(\mathbf{X}) \mathbf{a}(\mathbf{X}), \quad (1)$$

$$\mathbf{P}(\mathbf{X})$$

$$= [1, x, y, x^2, xy, y^2, \dots, x^m, x^{m-1}y, xy^{m-1}, y^m], \quad (2)$$

where, $a_i(\mathbf{X})$ is the vector of coefficients and $\mathbf{P}(\mathbf{X})$ is the basis function; m is the order of basic function

and k is the total number of the basic function terms. In this paper, the basis function of the form $\mathbf{P}(\mathbf{X}) = [1, x, x^2]$ ($m = 2$ and $k = 3$) is used for one-dimensional problems and $\mathbf{P}(\mathbf{X}) = [1, x, y, x^2, xy, y^2]$ ($m = 2$ and $k = 6$) is used for two-dimensional problems. Weighted discrete L_2 norm function is defined by:

$$\mathbf{J} = \sum_{j=1}^{n_s} w_j (\mathbf{X} - \mathbf{X}_j) (\mathbf{P}^T(\mathbf{X}_j) \mathbf{a}(\mathbf{X}) - u_j^h)^2, \quad (3)$$

where, u_j^h is the nodal value of the function to be approximated of point j , n_s is the total number of nodes in the support domain of point j , and w_j is the weighted function. In this paper, a cubic spline weight function is used, as follows:

$$w_j(\bar{d}) = \begin{cases} \frac{2}{3} - 4\bar{d}^2 + 4\bar{d}^3 & \bar{d} \leq \frac{1}{2} \\ \frac{4}{3} - 4\bar{d} + 4\bar{d}^2 - \frac{4}{3}\bar{d}^3 & \frac{1}{2} \leq \bar{d} \leq 1 \\ 0 & \bar{d} \geq 1 \end{cases} \quad (4)$$

where $\bar{d} = \|\mathbf{X} - \mathbf{X}_j\|/d_{wj}$ and d_{wj} is the radius of the support domain of point j . The vector of coefficients can be calculated by minimizing Eq. (3) as follows:

$$\mathbf{u}(\mathbf{X}) = \mathbf{P}^T(\mathbf{X}) \mathbf{A}^{-1}(\mathbf{X}) \mathbf{B}(\mathbf{X}) \mathbf{u}^h, \quad (5)$$

where \mathbf{u}^h is the vector of nodal values of the functions to be approximated, as follows:

$$\mathbf{u}^h = [u_1^h, u_2^h, \dots, u_{n_s}^h], \quad (6)$$

and $\mathbf{A}(\mathbf{X})$ and $\mathbf{B}(\mathbf{X})$ are defined as:

$$\mathbf{A}(\mathbf{X}) = \sum_{j=1}^{n_s} w_j (\mathbf{X} - \mathbf{X}_j) \mathbf{P}(\mathbf{X}_j) \mathbf{P}^T(\mathbf{X}_j), \quad (7)$$

$$\mathbf{B}(\mathbf{X}) = [w_1(\mathbf{X} - \mathbf{X}_1) \mathbf{P}(\mathbf{X}_1), w_2(\mathbf{X} - \mathbf{X}_2) \mathbf{P}(\mathbf{X}_2), \dots, w_{n_s}(\mathbf{X} - \mathbf{X}_{n_s}) \mathbf{P}(\mathbf{X}_{n_s})]. \quad (8)$$

Eq. (5) is rewritten in the following form:

$$\mathbf{u}(\mathbf{X}) = \mathbf{N}^T(\mathbf{X}) \mathbf{u}^h, \quad (9)$$

where $\mathbf{N}^T(\mathbf{X})$ is named as the MLS shape function. In the solution of partial differential equations, it is often necessary to obtain the shape function derivatives. The first order derivatives of the MLS shape function can be obtained as follows:

$$\begin{aligned} \frac{d\mathbf{N}}{dx} &= \frac{d\mathbf{P}}{dx} \mathbf{A}^{-1} \mathbf{B} + \mathbf{P}^T \frac{d\mathbf{A}^{-1}}{dx} \mathbf{B} + \mathbf{P}^T \mathbf{A}^{-1} \frac{d\mathbf{B}}{dx}, \\ \frac{d\mathbf{N}}{dy} &= \frac{d\mathbf{P}}{dy} \mathbf{A}^{-1} \mathbf{B} + \mathbf{P}^T \frac{d\mathbf{A}^{-1}}{dy} \mathbf{B} + \mathbf{P}^T \mathbf{A}^{-1} \frac{d\mathbf{B}}{dy}, \end{aligned} \quad (10)$$

while the second order derivatives of the MLS shape functions, which are only required when second order derivatives are present in the governing differential equations, are obtained as follows:

$$\begin{aligned} \frac{d^2\mathbf{N}}{dx^2} &= \frac{d^2\mathbf{P}^T}{dx^2} \mathbf{A}^{-1} \mathbf{B} + \mathbf{P}^T \frac{d^2\mathbf{A}^{-1}}{dx^2} \mathbf{B} \\ &\quad + \mathbf{P}^T \mathbf{A}^{-1} \frac{d^2\mathbf{B}}{dx^2} + 2 \left(\frac{d\mathbf{P}^T}{dx} \frac{d\mathbf{A}^{-1}}{dx} \mathbf{B} \right. \\ &\quad \left. + \frac{d\mathbf{P}^T}{dx} \mathbf{A}^{-1} \frac{d\mathbf{B}}{dx} + \mathbf{P}^T \frac{d\mathbf{A}^{-1}}{dx} \frac{d\mathbf{B}}{dx} \right), \\ \frac{d^2\mathbf{N}}{dy^2} &= \frac{d^2\mathbf{P}^T}{dy^2} \mathbf{A}^{-1} \mathbf{B} + \mathbf{P}^T \frac{d^2\mathbf{A}^{-1}}{dy^2} \mathbf{B} \\ &\quad + \mathbf{P}^T \mathbf{A}^{-1} \frac{d^2\mathbf{B}}{dy^2} + 2 \left(\frac{d\mathbf{P}^T}{dy} \frac{d\mathbf{A}^{-1}}{dy} \mathbf{B} \right. \\ &\quad \left. + \frac{d\mathbf{P}^T}{dy} \mathbf{A}^{-1} \frac{d\mathbf{B}}{dy} + \mathbf{P}^T \frac{d\mathbf{A}^{-1}}{dy} \frac{d\mathbf{B}}{dy} \right), \\ \frac{d^2\mathbf{N}}{dxy} &= \frac{d^2\mathbf{P}^T}{dxy} \mathbf{A}^{-1} \mathbf{B} + \mathbf{P}^T \frac{d^2\mathbf{A}^{-1}}{dxy} \mathbf{B} \\ &\quad + \mathbf{P}^T \mathbf{A}^{-1} \frac{d^2\mathbf{B}}{dxy} + \frac{d\mathbf{P}^T}{dx} \frac{d\mathbf{A}^{-1}}{dy} \mathbf{B} \\ &\quad + \frac{d\mathbf{P}^T}{dx} \mathbf{A}^{-1} \frac{d\mathbf{B}}{dy} + \frac{d\mathbf{P}^T}{dy} \frac{d\mathbf{A}^{-1}}{dx} \mathbf{B} \\ &\quad + \mathbf{P}^T \frac{d\mathbf{A}^{-1}}{dx} \frac{d\mathbf{B}}{dy} + \frac{d\mathbf{P}^T}{dy} \mathbf{A}^{-1} \frac{d\mathbf{B}}{dx} \\ &\quad + \mathbf{P}^T \frac{d\mathbf{A}^{-1}}{dy} \frac{d\mathbf{B}}{dx}. \end{aligned} \quad (11)$$

3. Mixed discrete least square formulation for solving quadratic PDE equations

In this section, the MDLSM method for the solution of quadratic PDEs is formulated. Consider the following two-dimensional quadratic PDE equation:

$$\begin{aligned} a \left(\frac{\partial^2 T}{\partial x^2} \right) + b \left(\frac{\partial^2 T}{\partial x \partial y} \right) + c \left(\frac{\partial^2 T}{\partial y^2} \right) + d \left(\frac{\partial T}{\partial x} \right) \\ + e \left(\frac{\partial T}{\partial y} \right) + f(T) = g \quad \text{on } \Omega, \end{aligned} \quad (12)$$

where, a , b , c , d , e , f and g are functions of x and y , and Ω is the domain of the problem. The equation is subject to the following Dirichlet and Neumann boundary conditions:

$$T = \bar{T} \quad \text{on } \Gamma_u, \quad (13)$$

$$\frac{\partial T}{\partial n} = \bar{q} \quad \text{on } \Gamma_t, \quad (14)$$

in which \bar{T} and \bar{q} are prescribed Dirichlet and Neumann boundary conditions on Γ_u and Γ_t boundaries, respectively.

Using the following definition of derivatives,

$$\begin{cases} \frac{\partial T}{\partial x} = q_x \\ \frac{\partial T}{\partial y} = q_y \end{cases} \quad (15)$$

Eq. (12) can be written using Eq. (15) as follows:

$$\begin{aligned} a \left(\frac{\partial q_x}{\partial x} \right) + b \left(\frac{\partial q_x}{\partial y} \right) + c \left(\frac{\partial q_y}{\partial y} \right) + d(q_x) \\ + e(q_y) + f(T) = g \quad \text{on } \Omega. \end{aligned} \quad (16)$$

Eqs. (15) and (16) can now be used as a substitute for the original quadratic PDE, which is written in compact form as:

$$\mathbf{L}(\mathbf{u}) - \mathbf{H} = \mathbf{0}, \quad (17)$$

where $\mathbf{L}(\cdot)$ is the first order differential operator, defined as:

$$\mathbf{L}(\cdot) = \mathbf{A}(\cdot)_x + \mathbf{B}(\cdot)_y + \mathbf{C}(\cdot). \quad (18)$$

\mathbf{u} and \mathbf{H} are the vectors of unknowns and right hand side, respectively, which are defined as:

$$\mathbf{u} = [T, q_x, q_y]^T, \quad (19)$$

$$\mathbf{H} = [0, 0, g]^T. \quad (20)$$

And \mathbf{A} , \mathbf{B} and \mathbf{C} are coefficient matrices as follows:

$$\begin{aligned} \mathbf{A} &= \begin{bmatrix} 1 & 0 & 0 \\ 0 & 0 & 0 \\ 0 & a & 0 \end{bmatrix}, \quad \mathbf{B} = \begin{bmatrix} 0 & 0 & 0 \\ 1 & 0 & 0 \\ 0 & b & c \end{bmatrix}, \\ \mathbf{C} &= \begin{bmatrix} 0 & -1 & 0 \\ 0 & 0 & -1 \\ f & d & e \end{bmatrix}. \end{aligned} \quad (21)$$

The Dirichlet and Neumann boundary conditions originally defined by Eqs. (13) and (14) can also be written in a compact form, in terms of the new vector of unknowns, \mathbf{u} , as:

$$\mathbf{D}\mathbf{u} - \bar{\mathbf{u}} = \mathbf{0}, \quad (22)$$

where, \mathbf{D} and $\bar{\mathbf{u}}$ are defined as:

$$\mathbf{D} = \begin{bmatrix} 1 & 0 & 0 \\ 0 & n_x & n_y \end{bmatrix}, \quad \bar{\mathbf{u}} = [\bar{T} \quad \bar{q}]^T. \quad (23)$$

n_x and n_y are direction cosines of the outward unit normal vectors to the boundaries of the body at

boundary points. Now, the residuals of the differential equation and the corresponding boundary condition at a typical node, k , are defined as:

$$(\mathbf{R}_\Omega)_k = \mathbf{L}_k(\mathbf{u}_k) - \mathbf{H}_K \quad \text{on } \Omega, \quad (24)$$

$$(\mathbf{R}_\Gamma)_k = \mathbf{D}_k \mathbf{u}_k - \bar{\mathbf{u}}_K \quad \text{on } \Gamma, \quad (25)$$

where \mathbf{R}_Ω and \mathbf{R}_Γ are the domain and boundary residuals, respectively.

Using a penalty approach for the satisfaction of the boundary condition leads to the following least squares functional, defined as:

$$I = \sum_{K=1}^{n_t} (\mathbf{R}_\Omega^T)_k (\mathbf{R}_\Omega)_k + \alpha \sum_{k=1}^{n_b} (\mathbf{R}_\Gamma^T)_k (\mathbf{R}_\Gamma)_k (\mathbf{R}_\Gamma)^k, \quad (26)$$

where n_d is the number of nodes in the domain, n_b is the number of boundary nodes, and $n_t = n_d + n_b$. α is the penalty coefficient defined as a positive scalar constant with a large enough value in order to impose the essential boundary condition with the desired accuracy. The proper value of the penalty parameter is determined prior to the main calculation, via a trial and error process.

Minimizing the least square functional of Eq. (26), with respect to nodal parameters, \mathbf{U} , leads to:

$$\mathbf{K}\mathbf{U} = \mathbf{F}, \quad (27)$$

where:

$$\mathbf{K}_{ij} = \sum_{k=1}^{n_t} [\mathbf{L}(\mathbf{N}_i)]_k^T [\mathbf{L}(\mathbf{N}_j)]_k + \alpha \sum_{k=1}^{n_b} [\mathbf{D}\mathbf{N}_i]_k^T [\mathbf{D}\mathbf{N}_j]_k, \quad (28)$$

$$\mathbf{F}_i = \sum_{k=1}^{n_t} [\mathbf{L}(\mathbf{N}_i)]_k^T \mathbf{H}_k + \alpha \sum_{k=1}^{n_b} [\mathbf{D}\mathbf{N}_i]_k^T \bar{\mathbf{u}}_k. \quad (29)$$

And \mathbf{U} is the vector of unknown nodal parameters. The final stiffness matrix \mathbf{K} is sparse, square, symmetric and positive definite, which can be efficiently solved using proper solvers. Since the least squares functional constructed by the MDLSM method is a saddle-point problem, its solution method does not require satisfying the Ladyzhenskaya-Babuška-Brezzi (LBB) condition [37]. This means that the same MLS shape functions of the same order can be used to solve the problem without stability issues. Also, the order of required shape function derivatives is decreased by one order, thus, complex and costly second derivative calculation of the MLS functions (Eq. (11)) is avoided. In addition, the unknown gradients are obtained simultaneously, removing the need for some post processing. Furthermore, both the original Dirichlet and Neumann boundary conditions can now be enforced as a Dirichlet-type boundary condition requiring the specification of a single penalty parameter.

4. Numerical examples

In this section, the accuracy and efficiency of the MDLSM for the solution of one-dimensional (1-D) and two-dimensional (2-D) quadratic PDEs are tested against three benchmark examples, and the results are compared with the exact results and those of the DLSM method. The polynomial basis, \mathbf{P} , for the construction of MLS shape functions is considered as $\mathbf{P} = [1, x, x^2]$ for 1-D problems and $\mathbf{P} = [1, x, y, x^2, xy, y^2]$ for 2-D problems. The radius of the influence domain is calculated by $d_w = \beta d_k$, where β is a constant coefficient between 2 to 3, determined by trial-and-error procedures [12–20], d_k is the distance of the k th nearest point to the node under consideration and k is the number of terms in the polynomial basis, \mathbf{P} , used. A constant value of $\alpha = 10^8$ is used as the penalty coefficient in all benchmark examples for enforcing the boundary conditions.

An error indicator is also used to calculate the accuracy and convergence rate of the MDLSM and irreducible DLSM method, defined as:

$$\text{Error Norm} = \sqrt{\frac{(\mathbf{U}^{\text{exact}} - \mathbf{U}^{\text{num}})^T (\mathbf{U}^{\text{exact}} - \mathbf{U}^{\text{num}})}{(\mathbf{U}^{\text{exact}})^T (\mathbf{U}^{\text{exact}})}}, \quad (30)$$

where $\mathbf{U}^{\text{exact}}$ and \mathbf{U}^{num} are the vector of exact analytical and numerical solutions, respectively. A regular distribution of nodes is used to solve all benchmark problems. The effect of the irregularity of nodal distribution on the accuracy of the solution has already been discussed by Amani et al. [22] in elasticity problems. This experience shows that while the MDLSM method yields a better solution on regular nodal distribution, its accuracy and efficiency are marginally affected by irregular nodal distribution.

4.1. One-dimensional PDE

As a first example, the 1-D PDE is solved using the MDLSM method, and the solution is compared with the results of the irreducible DLSM method and the exact analytical solution. Consider the following 1-D PDE as follows:

$$A \frac{d^2 T}{dx^2} + F(x) = 0, \quad 0 \leq x \leq 1, \quad (31)$$

where, $A = 1$ and $F(x) = -(3.4\pi)^2 \sin(3.4\pi x)$. The boundary conditions are defined as:

$$\begin{cases} \bar{T}(x) = 0 & \text{on } x = 0 \\ \bar{T}(x) = -\sin(3.4\pi) & \text{on } x = 1 \end{cases} \quad (32)$$

The exact analytical solution for this problem can be found to be:

$$T^{\text{exact}}(x) = -\sin(3.4\pi x). \quad (33)$$

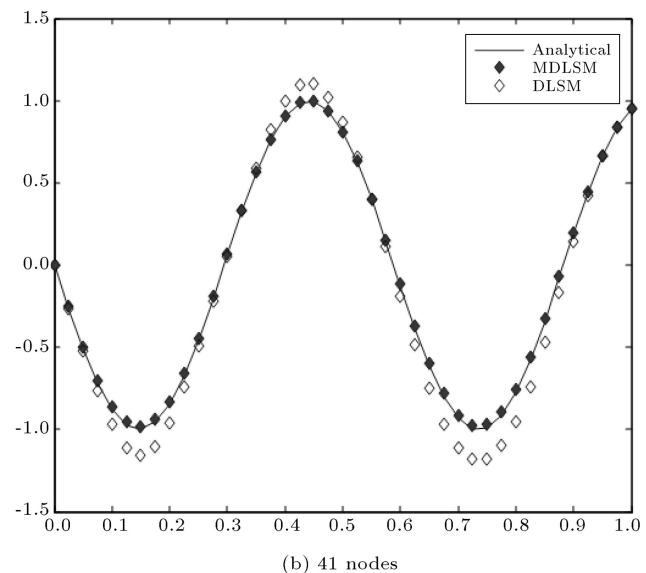
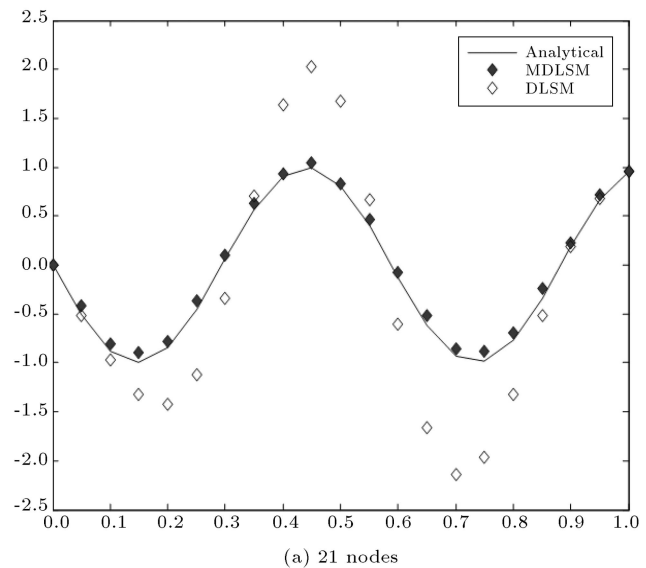
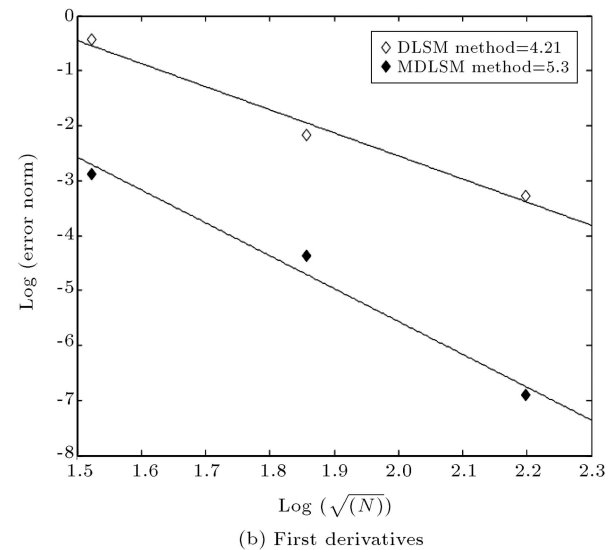
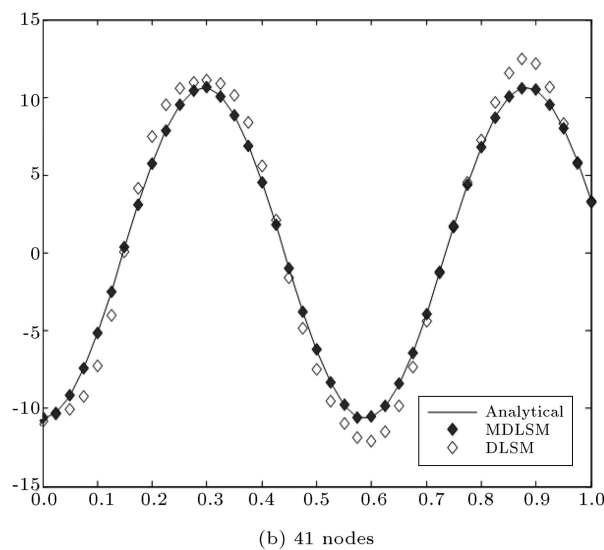
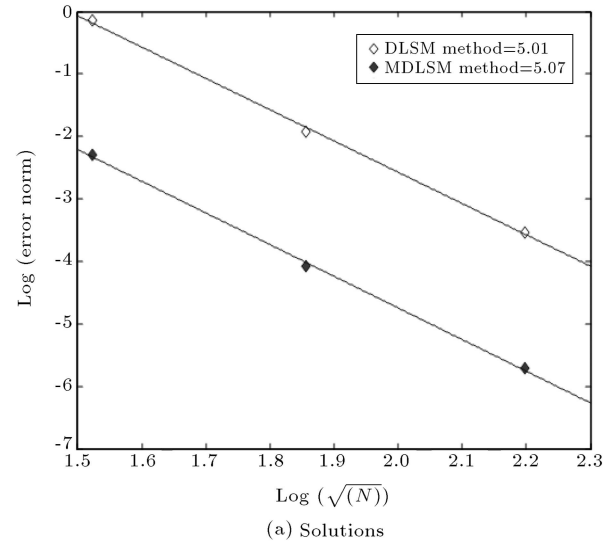
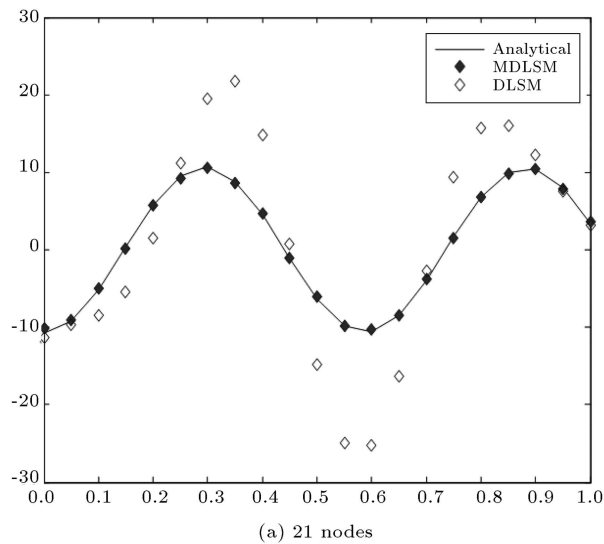


Figure 1. Numerical and analytical solutions for 1-D PDE.

The problem is solved on three different uniform nodal configurations, using 21, 41 and 81 nodes. Figure 1 compares the results of the MDLSM and the irreducible DLSM methods with the exact analytical solutions for two of the nodal configurations, while Figure 2 compares the first derivatives. It is clearly seen that the result obtained by the MDLSM method is more accurate than the irreducible DLSM method for the case considered. Table 1 compares the error norms obtained from MDLSM and irreducible DLSM methods on three nodal configurations. Also, to quantify the improvements made on the results of the mixed procedure, the convergence rate of the MDLSM method is compared with that of the irreducible DLSM method in Figure 3, indicating an increase of 0.06 and 1.11 in the rate of convergence for the solution and its first

Table 1. Comparing error norms of DLSTM and MDLSTM methods for 1-D PDE.

Number of nodes	DLSTM method (solutions)	MDLSTM method (solutions)	DLSTM method (first derivatives)	MDLSTM method (first derivatives)
21	1.3474	0.1110	0.6494	0.0567
41	0.0869	0.0286	0.1150	0.0126
81	0.0293	0.0033	0.0379	0.0010

**Figure 2.** Numerical and analytical first derivative of the solution for 1-D PDE.

derivatives, respectively. These results also show that the errors of the MDLSTM method are always less than those of the DLSTM method by two orders of magnitude, emphasizing the higher accuracy of the method.

4.2. Two-dimensional Poisson PDE

As a second example, the Poisson PDE is considered:

$$\frac{\partial^2 T}{\partial x^2} + \frac{\partial^2 T}{\partial y^2} = \sin(\pi x) \sin(\pi y), \quad 0 \leq x, \quad y \leq 1. \quad (34)$$

Figure 3. Convergence rate for 1-D PDE.

Subject to the following boundary conditions:

$$\bar{T}(x, y) = 0 \quad \text{on} \quad x = 0 \quad \text{and} \quad y = 0, \quad (35)$$

$$\begin{cases} \frac{\partial T}{\partial x} = \frac{1}{2\pi} \sin(\pi y) & \text{on} \quad x = 1 \\ \frac{\partial T}{\partial y} = \frac{1}{2\pi} \sin(\pi x) & \text{on} \quad y = 1 \end{cases} \quad (36)$$

The exact analytical solution of the problem can be defined as:

$$T^{\text{exact}}(x, y) = -\frac{1}{2\pi^2} \sin(\pi x) \sin(\pi y). \quad (37)$$

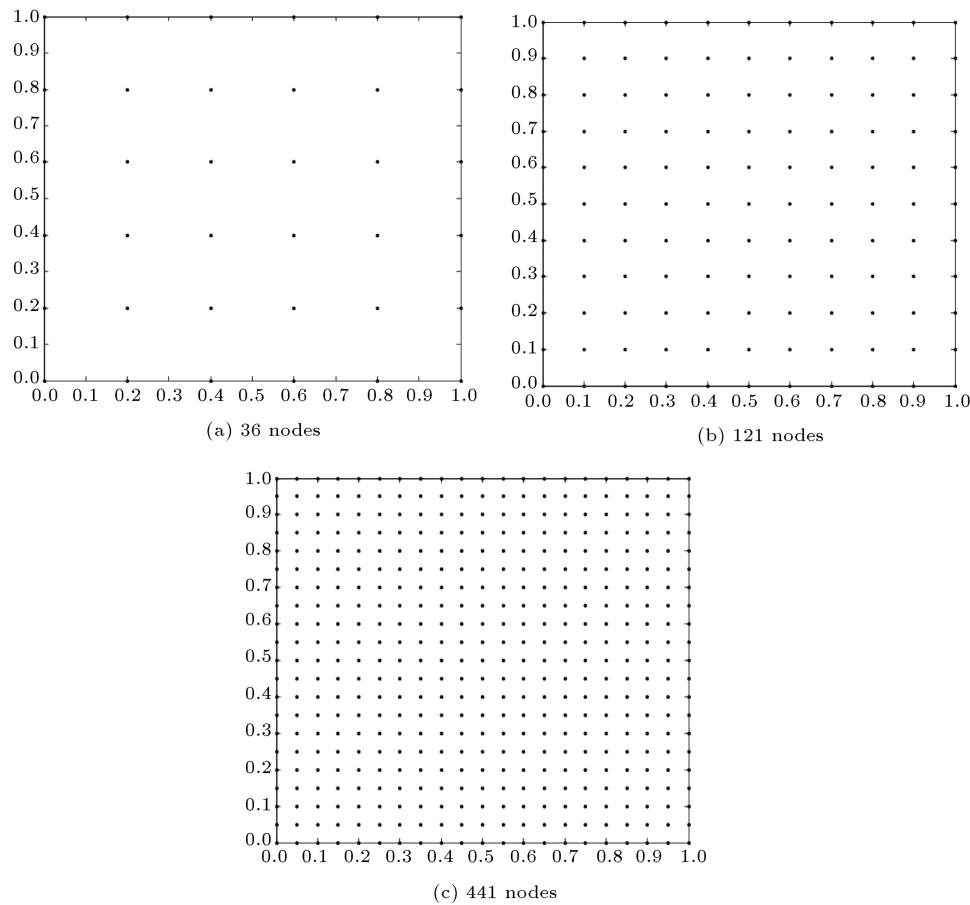


Figure 4. Nodal distribution for 2-D Poisson PDE.

Table 2. Comparison of error norms of DLSM and MDLSM methods for 2-D Poisson PDE.

Number of nodes	DLSM method (solutions)	MDLSM method (solutions)	DLSM method (first derivatives)	MDLSM method (first derivatives)
36	0.4302	0.1810	0.2598	0.0800
121	0.1697	0.0475	0.2088	0.0201
441	0.0339	0.0120	0.0656	0.0050

The domain is discretized using 36, 121 and 441 nodes, as shown in Figure 4. The solution obtained using MDLSM and its first and second derivatives is compared with irreducible DLSM and exact analytical methods in Figures 5-9 for nodal configurations of 121 and 441 nodes, indicating the higher accuracy of the MDLSM method. The convergence rate of the MDLSM method is compared with that of the irreducible DLSM method in Figure 10, using the error norms that are presented in Table 2, showing an increase of 0.14 and 1.1 in the convergence rate of the MDLSM method in comparison with an irreducible DLSM method for the solution and its first derivatives, respectively. It is again seen that the solutions obtained by the MDLSM method are more accurate than those of the DLSM method, by one order of magnitude.

4.3. Two-dimensional Laplace PDE

The Laplace equation is considered in the quarter circle domain of radius R with a quadrant hole of radius R_0 , as shown in Figure 11.

$$\frac{\partial^2 T}{\partial x^2} + \frac{\partial^2 T}{\partial y^2} = 0. \quad (38)$$

The boundary conditions considered are of the Dirichlet type, defined as:

$$\begin{cases} \bar{T} = A & \text{on } r = R \\ \bar{T} = A + B \left(\frac{R^2}{x} - x \right) & \text{and } x = 0 \\ \bar{T} = A + B \left(\frac{R^2}{R_0} - R_0 \right) \cos(\theta) & \text{on } y = 0 \\ \bar{T} = A + B \left(\frac{R^2}{R_0} - R_0 \right) \cos(\theta) & \text{on } r = R_0 \end{cases} \quad (39)$$

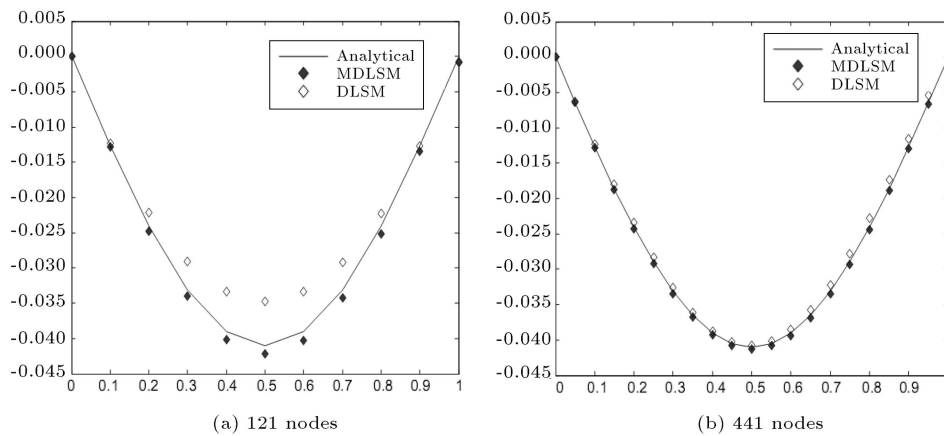


Figure 5. Numerical and analytical solutions for 2-D Poisson PDE on $y = 0.3$.

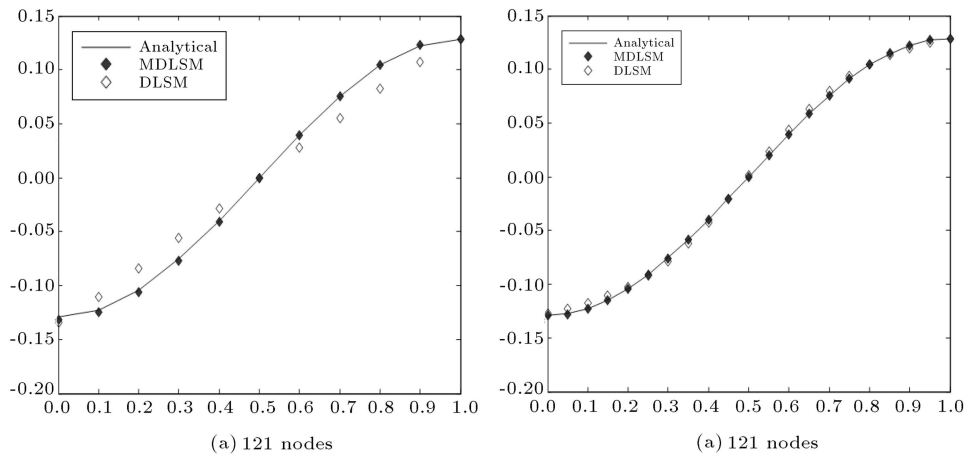


Figure 6. First derivative of solutions in x direction on $y = 0.3$ for 2-D Poisson PDE.

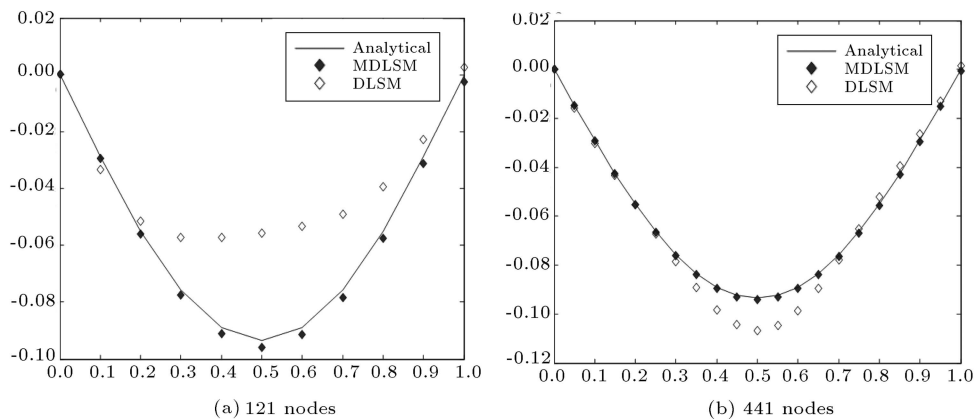


Figure 7. First derivative of solutions in y direction on $y = 0.3$ for 2-D Poisson PDE.

The exact analytical solution of the problem can be shown to be:

$$T^{\text{exact}} = A + B \left(\frac{R^2}{r} - r \right) \cos(\theta), \quad (40)$$

in which the values of the parameters, A and B , are set equal to unity. In this example, values of $R = 5$ and $R_0 = 1$ are used. Three nodal distributions with

29, 79 and 359 nodes, as illustrated in Figure 12, are used to solve the problem. Contours of solutions obtained by the MDLSM method are compared with those of the DLSM method and the exact analytical solutions (see Figure 13). The convergence rate of the MDLSM method is compared with that of the irreducible DLSM method in Figure 14, using the error norms listed in Table 3. The results show an

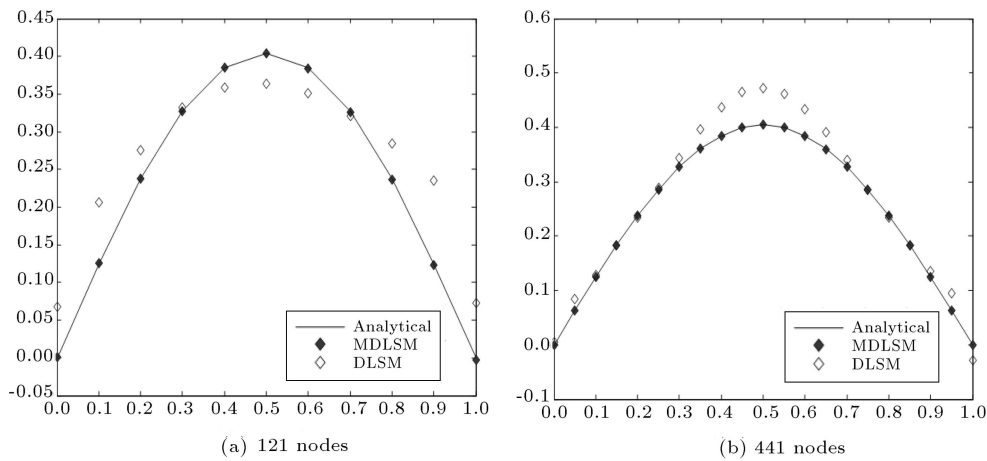


Figure 8. Second derivative of solutions in x direction on $y = 0.3$ for 2-D Poisson PDE.

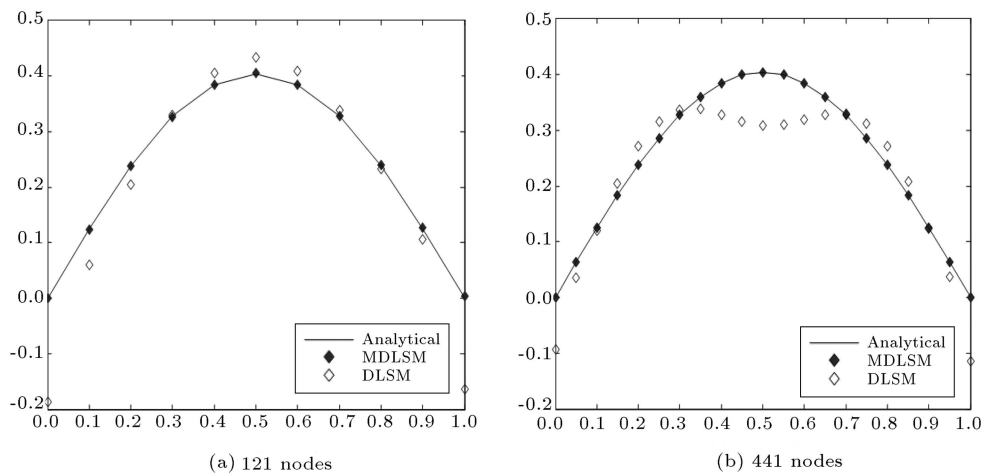


Figure 9. Second derivative of solutions in y direction on $y = 0.3$ for 2-D Poisson PDE.

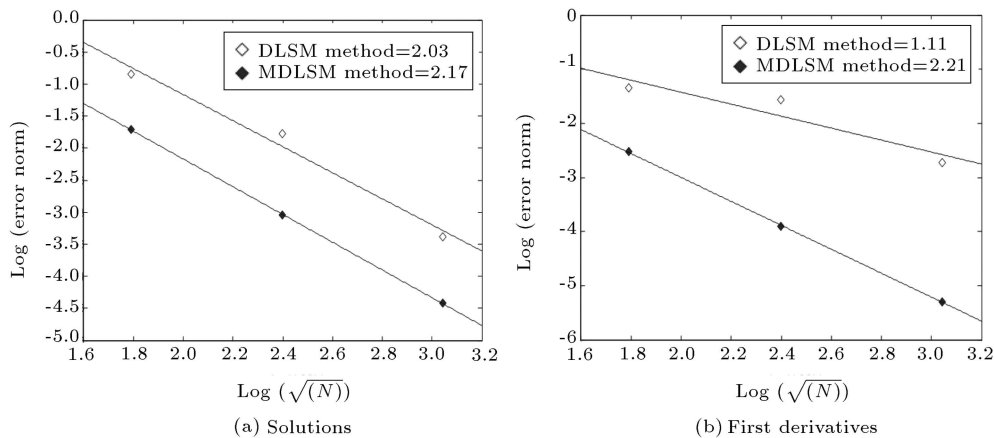


Figure 10. Convergence rate for 2-D Poisson PDE.

increase of 0.45 and 0.96 in the convergence rate of the MDLSM method in comparison with the irreducible DLSM method for the solution and its first derivatives, respectively; the solutions of MDLSM being more accurate than those of DLSM by 1.5 orders of magnitude.

5. Conclusion

In this paper, the MDLSM method was used for the solution of quadratic partial differential equations. The MDLSM method was formulated based on minimization of the least square functional, formed as the sum

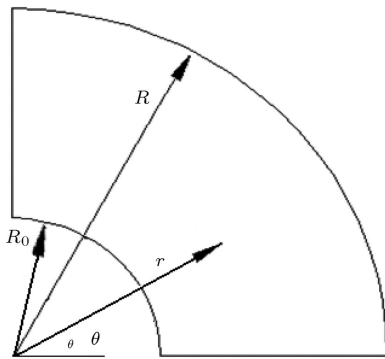
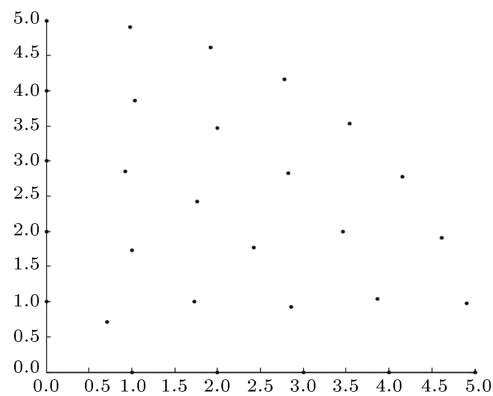
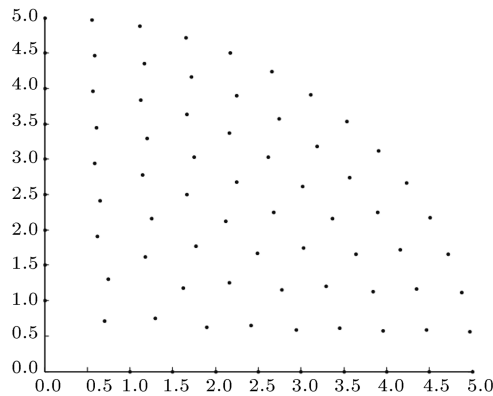


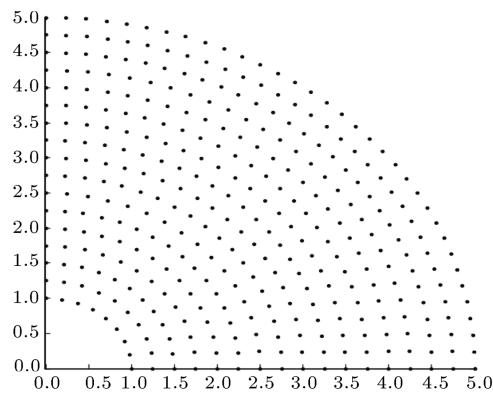
Figure 11. Quarter circle domain with a quadrant hole.



(a) 29 nodes

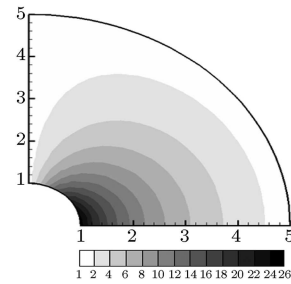


(b) 79 nodes

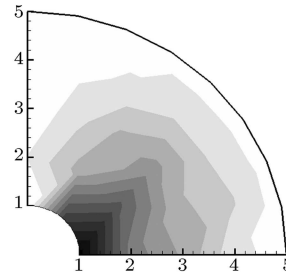


(c) 359 nodes

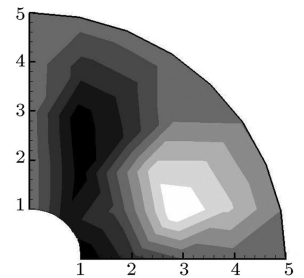
Figure 12. Nodal distribution for 2-D Laplace PDE.



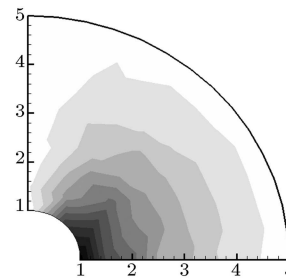
(a) Exact analytical solution



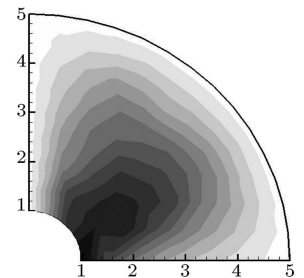
(b) MDLSM with 29 nodes



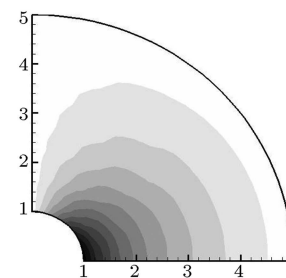
(c) DLSDM with 29 nodes



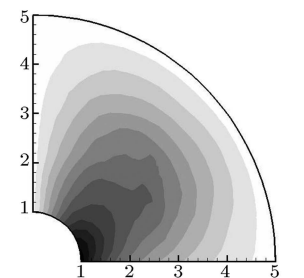
(d) MDLSM with 79 nodes



(e) DLSDM with 79 nodes



(f) MDLSM with 359 nodes



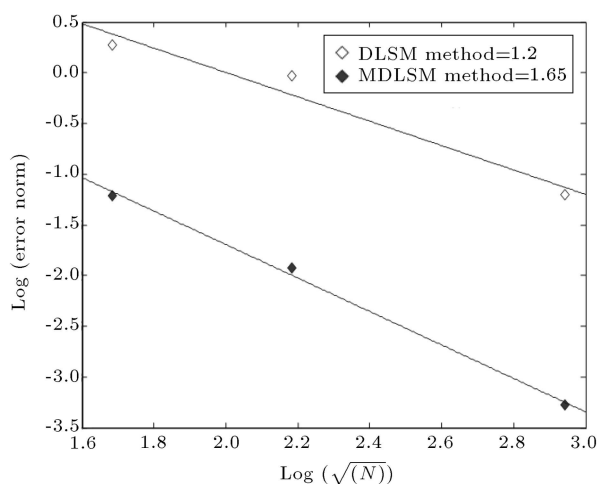
(g) DLSDM with 359 nodes

Figure 13. Contours of MDLSM and DLSDM methods for 2-D Laplace PDE.

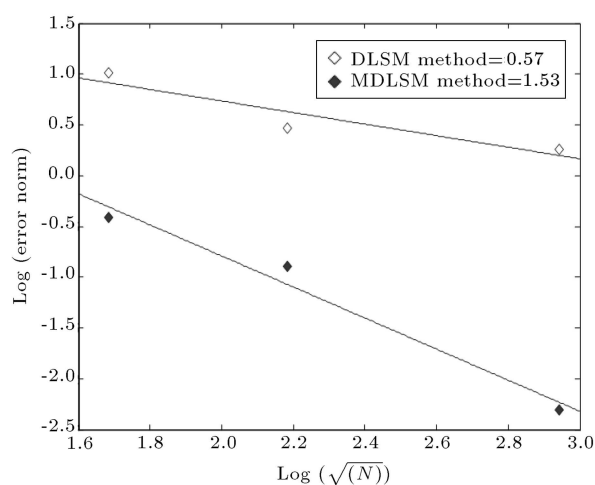
of the residuals of the differential equation and its boundary conditions at nodal points. The penalty approach was used to impose the Dirichlet-type boundary conditions. The main unknown parameter and its first derivatives were approximated independently and simultaneously with the same MLS shape functions, without requiring satisfying the LBB condition. Also, the required order of MLS shape functions derivatives was decreased by one order, removing the need for complex and costly second derivative calculation of the MLS shape functions. Three benchmark examples

Table 3. Comparison of error norms of DLISM and MDLISM methods for 2-D Laplace PDE.

Number of nodes	DLISM method (solutions)	MDLISM method (solutions)	DLISM method (first derivatives)	MDLISM method (first derivatives)
29	1.3141	0.2965	2.7453	0.6601
79	0.9670	0.1458	1.6032	0.4122
359	0.301	0.0377	1.1592	0.1168



(a) Solutions



(b) First derivatives

Figure 14. Convergence rate for 2-D Laplace PDE.

from quadratic PDEs were solved, and the results were produced and compared with those of the irreducible DLISM method and the exact analytical solutions. The results indicated the higher accuracy of the MDLISM method compared with the irreducible DLISM method, represented by an increase in the convergence rate of the MDLISM method. While the MDLISM method was used to solve linear PDEs in this paper, the method can be easily extended to solve nonlinear problems with no special treatment. In nonlinear cases, the final linear system of equations would be replaced by nonlinear ones which can be easily solved using iterative methods.

References

1. Afshar, M.H., Naisipour, M. and Amani, J. "Node moving adaptive refinement strategy for planar elasticity problems using Discrete Least Squares meshless method", *Finite Elem. Anal. Des.*, **47**(12), pp. 1315-1325 (2011).
2. Gingold, R.A. and Monaghan, J.J. "Smoothed particle hydrodynamics-theory and application to non-spherical stars", *Mon. Not. R. Astron. Soc.*, **181**, pp. 375-389 (1977).
3. Belytschko, T., Lu, Y.Y. and Gu, L. "Element-free Galerkin methods", *Int. J. Numer. Meth. Eng.*, **37**(2), pp. 229-256 (1994).
4. Belytschko, T., Krongauz, Y., Organ, D., Fleming, M. and Krysl, P. "Meshless methods: An overview and recent developments", *Comput. Methods Appl. Mech. Engrg.*, **139**(1), pp. 3-47 (1996).
5. Atluri, S. and Zhu, T. "A new meshless local Petrov-Galerkin (MLPG) approach in computational mechanics", *Comput. Mech.*, **22**(2), pp. 117-127 (1998).
6. Atluri, S. and Zhu, T.L. "The meshless local Petrov-Galerkin (MLPG) approach for solving problems in elasto-statics", *Comput. Mech.*, **25**(2), pp. 169-179 (2000).
7. Lin, H. and Atluri, S. "Meshless local Petrov-Galerkin (MLPG) method for convection diffusion problems", *Comput. Model. Eng. Sci.*, **1**(2), pp. 45-60 (2000).
8. Mahmoodabadi, M.J., AbedzadehMaafi, R., Bagheri, A. and Baradaran, G.H. "Article meshless local Petrov-Galerkin method for 3D steady-state heat conduction problems", *Advances in Mechanical Engineering*, p. 10 (2011).
9. Liu, W.K., Jun, S. and Zhang, Y.F. "Reproducing kernel particle methods", *Int. J. Numer. Meth. Fl.*, **20**(8-9), pp. 1081-1106 (1995).
10. Zhu, T., Zhang, J.D. and Atluri, S. "A local boundary integral equation (LBIE) method in computational mechanics, and a meshless discretization approach", *Comput. Mech.*, **21**(3), pp. 223-235 (1998).
11. Atluri, S., Sladek, J., Sladek, V. and Zhu, T. "The local boundary integral equation (LBIE) and its meshless implementation for linear elasticity", *Comput. Mech.*, **25**, pp. 180-198 (2000).
12. Liszka, T.J., Duarte, C.A.M. and Tworzydło, W.W.

- “Hp-meshless cloud method”, *Comput. Methods Appl. Mech. Engrg.*, **139**, pp. 263-288 (1996).
13. Onate, E., Perazzo, F. and Miquel, J. “A finite point method for elasticity problems”, *Comput. Struct.*, **79**, pp. 2151-2163 (2001).
 14. Arzani, H. and Afshar, M.H. “Solving Poisson’s equations by the discrete least square meshless method”, *WIT Trans. Model. Simul.*, **42**, pp. 23-31 (2006).
 15. Firoozjaee, A.R. and Afshar, M.H. “Discrete least squares meshless method with sampling points for the solution of elliptic partial differential equations”, *Eng. Anal. Bound. Elem.*, **33**(1), pp. 83-92 (2009).
 16. Afshar, M.H., Lashckarbolok, M. and Shobeyri, G. “Collocated discrete least squares meshless (CDLSM) method for the solution of transient and steady-state hyperbolic problems”, *Int. J. Numer. Meth. Fl.*, **60**(10), pp. 1055-1078 (2009).
 17. Afshar, M.H. and Firoozjaee, A.R. “Adaptive simulation of two dimensional hyperbolic problems by collocated discrete least squares meshless method”, *Comput. Fluids*, **39**(10), pp. 2030-2039 (2010).
 18. Firoozjaee, A.R. and Afshar, M.H. “Steady-state solution of incompressible Navier-Stokes equations using discrete least-squares meshless method”, *Int. J. Numer. Meth. Fl.*, **67**(3), pp. 369-382 (2011).
 19. Naisipour, M., Afshar, M.H., Hassani, B. and Firoozjaee, A.R. “Collocation discrete least square (CDLS) method for elasticity problems”, *Int. J. Civil Eng.*, **7**, pp. 9-18 (2009).
 20. Afshar, M.H. and Lashckarbolok, M. “Collocated discrete least-squares (CDLS) meshless method: Error estimate and adaptive refinement”, *Int. J. Numer. Meth. Fl.*, **56**(10), pp. 1909-1928 (2008).
 21. Afshar, M.H., Amani, J. and Naisipour, M. “A node enrichment adaptive refinement by discrete least squares meshless method for solution of elasticity problems”, *Eng. Anal. Bound. Elem.*, **36**(3), pp. 385-393 (2012).
 22. Amani, J., Afshar, M.H. and Naisipour, M. “Mixed discrete least squares meshless method for planar elasticity problems using regular and irregular nodal distributions”, *Eng. Anal. Bound. Elem.*, **36**(5), pp. 894-902 (2012).
 23. Zienkiewicz, O., Qu, S., Taylor, R. and Nakazawa, S. “The patch test for mixed formulations”, *Int. J. Numer. Meth. Eng.*, **23**(10), pp. 1873-1883 (1986).
 24. Zienkiewicz, O. and Taylor, R., *The Finite Element Method*, **2**, McGraw-Hill (2000).
 25. Papadopoulos, P. and Taylor, R.L. “A mixed formulation for the finite element solution of contact problems”, *Comput. Methods Appl. Mech. Engrg.*, **94**(3), pp. 373-389 (1992).
 26. Pitkaranta, J. and Stenberg, R. “Analysis of some mixed finite element methods for plane elasticity equations”, *Math. Comput.*, **41**(164), pp. 399-423 (1983).
 27. Raviart, P. and Thomas, J. “A mixed finite element method for 2nd order elliptic problems”, *Proc. Conf., Consiglio Naz. delle Ricerche (C.N.R.)*, Rome (1975), Springer, Berlin, pp. 292-315, *Lecture Notes in Math. Aspects of finite elem. Meth.*, **606** (1977).
 28. Tchonkova, M. and Sture, S. “A mixed least squares method for solving problems in linear elasticity: Formulation and initial results”, *Comput. Mech.*, **19**(4), pp. 317-326 (1997).
 29. Atluri, S., Liu, H. and Han, Z. “Meshless local Petrov-Galerkin (MLPG) mixed collocation method for elasticity problems”, *Comput. Model. Eng. Sci.*, **4**(3), p. 141 (2006).
 30. Soric, J. and Jarak, T. “Mixed meshless formulation for analysis of shell-like structures”, *Comput. Methods Appl. Mech. Engrg.*, **199**(17-20), pp. 1153-1164 (2010).
 31. Liu, G.R. and Gu, Y.T., *An Introduction to mesh-free Methods and their Programming*, Springer Verlag (2005).
 32. Gu, L. “Moving kriging interpolation and element-free Galerkin method”, *Int. J. Numer. Meth. Eng.*, **56**(1), pp. 1-11 (2003).
 33. Sukumar, N., Huang, Z., Prévost, J.H. and Suo, Z. “Partition of unity enrichment for bimaterial interface cracks”, *Int. J. Numer. Meth. Eng.*, **59**(8), pp. 1075-1102 (2004).
 34. Sukumar, N. “Construction of polygonal interpolants: A maximum entropy approach”, *Int. J. Numer. Meth. Eng.*, **61**, pp. 2159-2181 (2004).
 35. Arroyo, M. and Ortiz, M. “Local maximum-entropy approximation schemes: A seamless bridge between finite elements and meshfree methods”, *Int. J. Numer. Meth. Eng.*, **65**(13), pp. 2167-2202 (2006).
 36. Lancaster, P. and Salkauskas, K. “Surfaces generated by moving least squares methods”, *Math. Comput.*, **37**(155), pp. 141-158 (1981).
 37. Brezzi, F. and Fortin, M., *Mixed and Hybrid Finite Element Methods*, New York: Springer (1991).

Biographies

Saeb Faraji was born in Jolfa, Iran, in 1986. He received his BS degree in Civil Engineering from the University of Urmia, Iran, in 2009, and his MS degree (honors) in Structural and Hydraulic Engineering, in 2012, from Iran University of Science and Technology (IUST), Tehran, Iran. He is author or coauthor of 3 research articles, which have been published in refereed conference papers. His research interests include numerical simulation and refinement procedures focusing on meshless and finite element methods and their applications in elasticity and fluid problems.

Mohammad Hadi Afshar obtained his BS in Civil Engineering from Tehran University, Iran, in 1984, and his MS and PhD degrees at University College of Swansea, Wales, UK, in 1993. He is now Associate Professor in the Civil Engineering Department at Iran University of Science and Technology, Tehran, Iran. He has published more than 80 journal papers and 60 conference papers. His research interests include numerical modeling of elasticity and fluid mechanic problems.

Jafar Amani was born in Ardabil, Iran, in 1985. He received his BS degree from the Civil Engineering Department at the University of Mohaghegh Ardabili (UMA), Iran, in 2007, and his MS degree (honors) in Structural and Hydraulic Engineering, in 2009, from Iran University of Science and Technology (IUST), Tehran, Iran, where he is currently a PhD degree student of Civil Engineering. He is author/coauthor of 5 research articles that have been published in international journals and 9 refereed conference papers.